SUPPLEMENTAL MATERIAL

Additional Methods

Flow cytometry. The following fluorochrome labeled mAb were used: phycoerythrin-CyChrome7 (PE-CyTM7)-anti CD14, allophycocyanin (APC)-Cy7-anti CD16, peridinin-chlorophyll-protein (PerCP)-Cy5.5-anti HLA-DR, PE-anti CD11b, APC-anti CD11c, APC-anti CD18, APC-anti CD29, fluorescein isothiocyanate (FITC)-anti CD32, APC-anti CD36, PE-anti CD62L, APC-anti CD192 (CCR2), FITC-anti CD195 (CCR5) [all from BD Biosciences, San Jos, CA, USA]; PE-anti CD204 (SR-A) [R&D systems, Abingdon, UK] and PE-anti CD197 (CCR7) [Biolegend, SanDiego, CA, USA]. Samples were incubated for 20 min at RT in the dark. To lyse red blood cells, 700 μL of PharmLyse1 (BD Biosciences, San Jose, CA) was added for 12 min, after which the samples were centrifuged at 400g for 5 min, the supernatant discarded and the samples resuspended in 400 μL of staining buffer. All data were collected on a FACS Calibur (Becton Dickinson, NJ), compensation was performed using single color fluorochromes and BD FacsComp beads, and samples were analyzed using FlowJo software (version 5.4+); for gating strategy and representative histograms see **Figure S3**. Delta mean fluorescence intensity (MFI) was obtained by subtracting median MFI from the isotype from the median MFI of the marker in corresponding color. Please note that the delta MFI values of CD62L were scaled down by a factor 10.000 to fit the bar graph.

Lipid Extraction. The lipids were extracted by the method previously described by Folch *et al.* with modifications.[1, 2] The lipid extracts were stored in CM (2:1), flushed with nitrogen, capped and stored at -80^{0}C till analysis. The internal standard mixture spiked into each sample prior to extraction consisted of 1,2-dinonanoyl-*sn*-glycero-3-phosphocholine (DNPC), 1-heptadecanoyl-

2-hydroxy-*sn*-glycero-3-phosphocholine (17:0 LPC)[3]. Synthetic 1-palmitoyl-2-(5-oxovaleroyl)-sn-glycero-3-phosphocholine (POVPC), 1-palmitoyl-2-glutaroyl- sn -glycero-3-phosphocholine (PGPC), 1-palmitoyl-2-azelaoyl-sn-glycero-3-phosphocholine (PAzPC), and 1-palmitoyl-2-(9'-oxo-nonanoyl)-sn-glycero-3-phosphocholine were purchased from Avanti Polar Lipids (Alabaster, AL). 1-palmitoyl-2-(4-keto-dodec-3-ene-dioyl) phosphatidylcholine (KDdiA-PC) were from Cayman Chemicals (Ann Arbor, MI)

HPLC. The detection of oxidized PCs were carried out in reverse-phase (RP) chromatography as reported previously[2, 4-7]. Briefly lipid extracts were reconstituted in an RP solvent system consisting of Acetonitrile-Isopropanol-Water (65:30:5 vol/vol/vol). Thirty microliters of the sample was injected on to Ascentis Express C18 HPLC column (15cmx2.1mm, 2.7µm; Supelco Analytical, Bellefonte, Pennsylvania, USA) and using a Prominence UFLC system from Shimadzu Corporation (Canby, Oregon, USA). Elution was performed by linear gradient of solvent A (Acetonitrile/Water, 60:40 vol/vol) and solvent B (Isopropanol/Acetonitrile, 90:10, vol/vol) both the solvents containing 10 mM ammonium formate and 0.1% formic acid. The time program used was as follows: initial solvent B at 32% until 4.00 min; switched to 45% B; 5.00 min 52% B; 8.00 min 58% B; 11.00 min 66% B; 14.00 min 70% B; 18.00 min 75% B; 21.00 min 97% B; 25.00 min 97% B; 25.10 min 32% B until the elution was stopped at 30.10 min. A flow rate of 260 µl/min was used for analysis, and the column and sample tray were held at 45 and 4˚C, respectively.

Mass Spectrometry. The HPLC system was coupled to 4000 QTRAP® triple quadrupole mass spectrometer system with a Turbo V electrospray ion source from AB Sciex (Framingham, Massachusetts, USA). For phosphatidylcholine, the detection was carried out in positive ion

mode by MRM of 6 transitions using PC-specific product ion (184.3 *m/z*, Da), which corresponds to the cleaved phosphatidylcholine. The MRM settings were as follows: declustering potential=125, entrance potential=10, collision energy=53, collision cell exit potential=9 and dwell time= 50 msec. [8, 9]

For each synthetic OxPL, POVPC, PGPC, PONPC, PAzPC and KDdiA-PC external calibration (i.e., using plasma-free standard solutions) was carried out to estimate linear range and sensitivity for these analytes and relative ionization compared to DNPC at equimolar levels. Concentrations of analytes were determined from calibration curves (1/x weighted linear regression) plotted as ratio of analyte peak area/DNPC peak area versus the amount of analyte on a column. The instrument was tuned by direct infusion of poly(propylene glycol) (PPG) in both positive and negative modes and external mass calibration was performed at regular intervals. Retention time window in MRM was set to detect peaks of significance within 60 seconds of confirmed retention time and data was collected utilizing Analyst® Software 1.6 (AB Sciex). Multi-quant® Software 2.1 (AB Sciex) was used to compare peak areas of internal standards and unknown analytes to quantitate the results.

Additional Figures

Fig. S1. Schematic of lipoprotein(a)

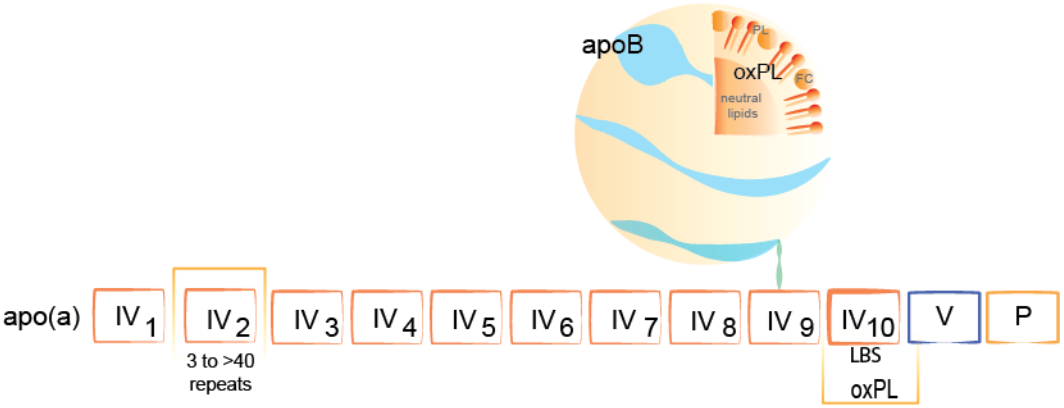

Lipoprotein (a) [Lp(a)] is composed of apolipoprotein(a) [apo(a)] covalently linked to apolipoprotein B-100 (apoB) of LDL. This LDL contains a central core of neutral lipids, surface phospholipids (PL) and free cholesterol (FC). Apo(a) comprises an inactive protease domain (P) and a series of loop structures termed kringle (K), including KIV type 2, (KIV_2) which is present in 3 to >40 copies. Genes encoding an apo(a) allele with smaller numbers of KIV_2 repeats lead to higher levels of Lp(a) in plasma, presumably due to higher rates of hepatic synthesis. Phosphocholine containing oxidized phospholipids (OxPL) are present in the lipid phase and covalently bound to apo(a) in the areas near KIV-10 and KV.

Fig. S2. Arterial wall dimensions assessed with MR imaging

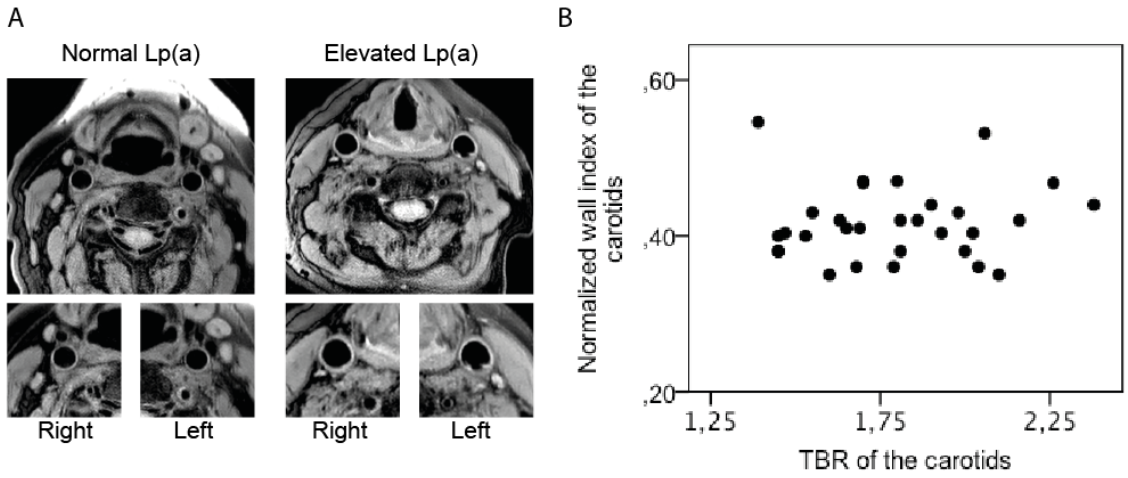

(**A**) Cross-sectional MR images used to quantify the arterial wall dimension, expressed as the normalized wall index (NWI), of the carotid arteries of normal Lp(a) and elevated Lp(a) subjects, (**B**) scatterplot illustrating no correlation between the arterial wall dimension (NWI, normalized wall index) and inflammation (TBR, target to background ratio, as assessed with ^{18}F-FDG PET/CT) in subjects with elevated Lp(a).

Fig. S3. Gating strategy to define monocyte population and representative histograms

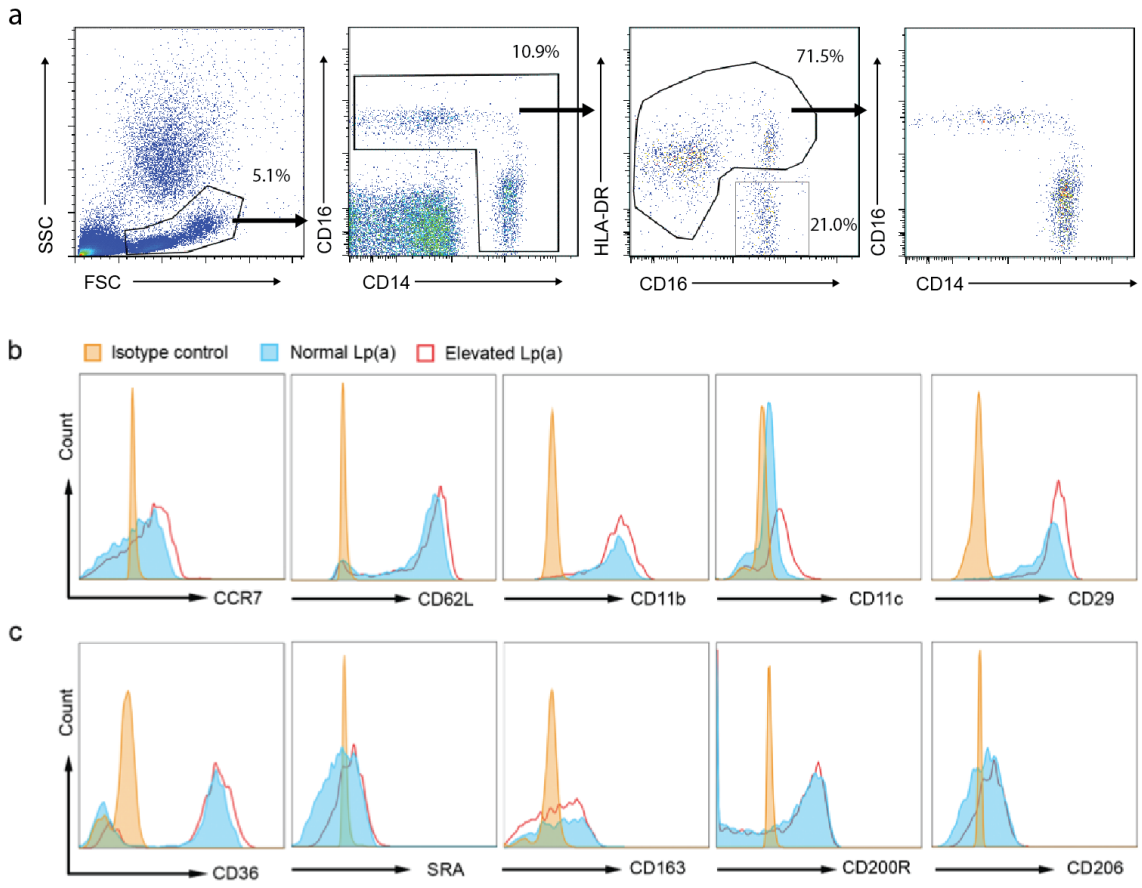

(A) The monocyte population was gated as follows; the leukocyte population was gated on a forward side scatter and subsequently viewed on a CD14/CD16 plot in which the $CD14^{pos}CD16^{pos}$ cell cloud was gated, after which these cells were then shown on the CD16/HLA-DR plot to exclude the $HLA\text{-}DR^{neg}CD16^{pos}$ cells. For gating graphs log scale was used, percentages of cells in gates are shown. Cells were analyzed using FlowJo software (version 5.4+). **(B)** Representative FACS histograms (of Figure 2A) show the expression of chemokine, adhesion and transmigration markers and (**C**) the expression of scavenger and other receptors (Figure 2D) on monocytes as assessed by flow cytometry of subjects with elevated Lp(a) (red line) compared with subjects with normal Lp(a) (blue line). The isotype control

(orange line) was similar between the two groups and therefore only one isotype control is showed.

Fig. S4. Monocytes of Lp(a) subjects have an increased response to LPS

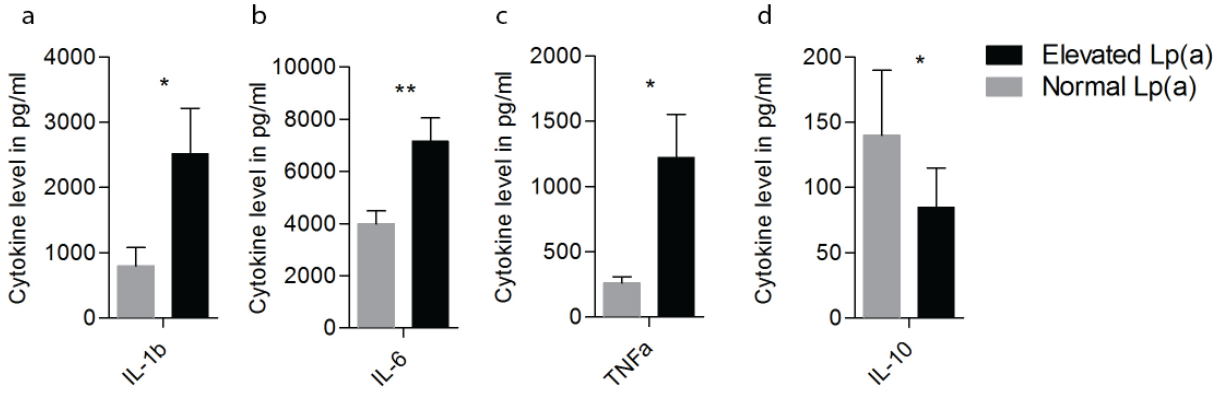

In response to an overnight challenge to LPS (10 ng/ml) monocytes isolated from subjects with elevated Lp(a) (black bars, n=15) produced higher levels of TNFα, IL-1β and IL-6 and lower levels of IL-10, compared to monocytes of subjects with normal Lp(a) (grey bars, n=15).

**=p<0.05, **=p<0.01.*

Fig. S5. Levels of OxPC molecules identified in human Lp(a)

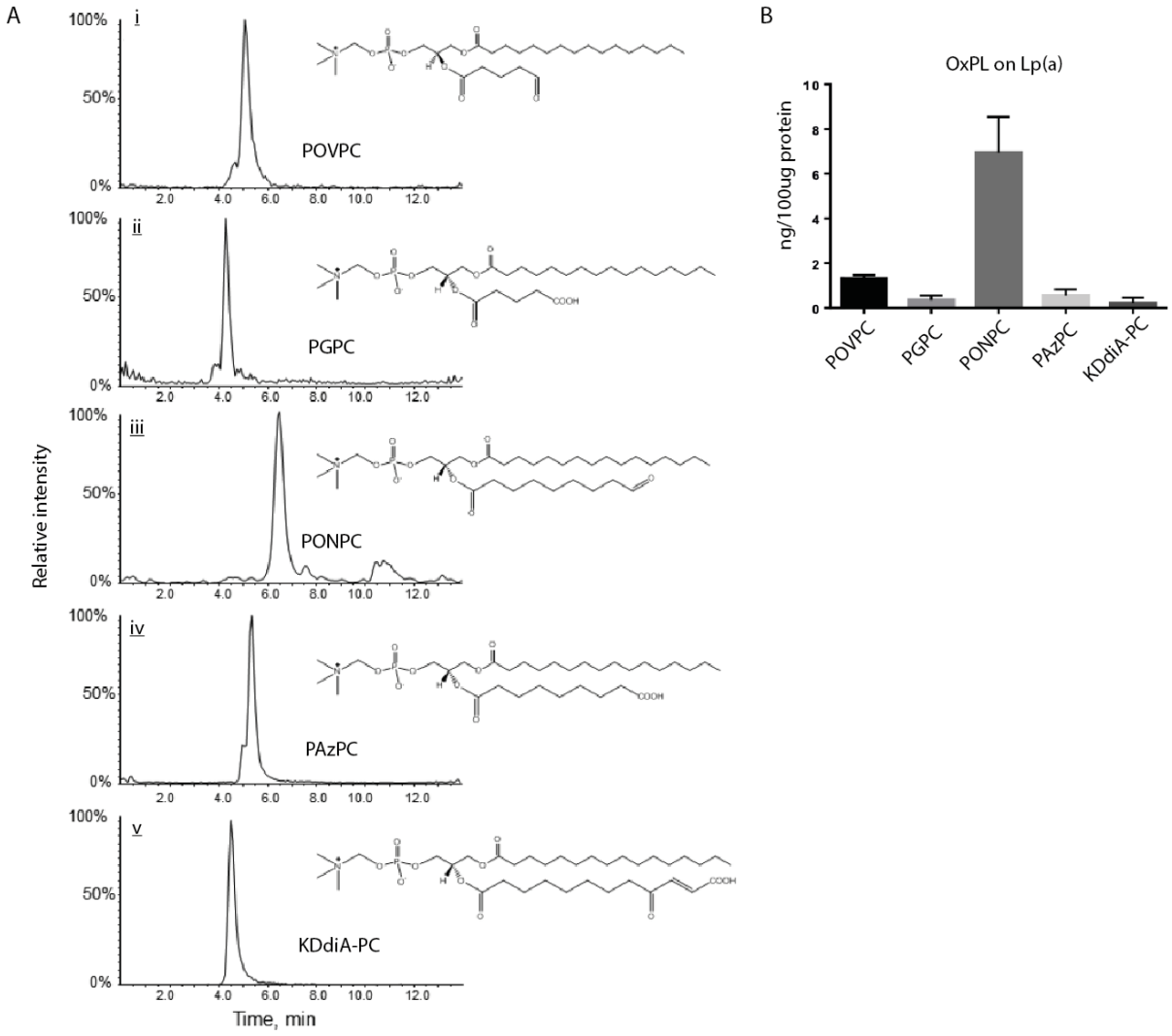

Quantitation was based on internal standard DNPC, details are given in methods. (**A**) Identification of oxPC molecules on human Lp(a). Single ion plots of MRM analysis of human Lp(a) lipid extract. Reversephase separation of the most abundant fragmented OxPC products (i)POVPC, (ii) PGPC, (iii) PONPC, (iv) PAzPC, (v) KDdiA-PC (n=3), and (**B**) quantification of oxPC molecules on human Lp(a) (n=3).

Fig. S6. Lp(a) and its OxPL load induce an enhanced monocyte response to LPS

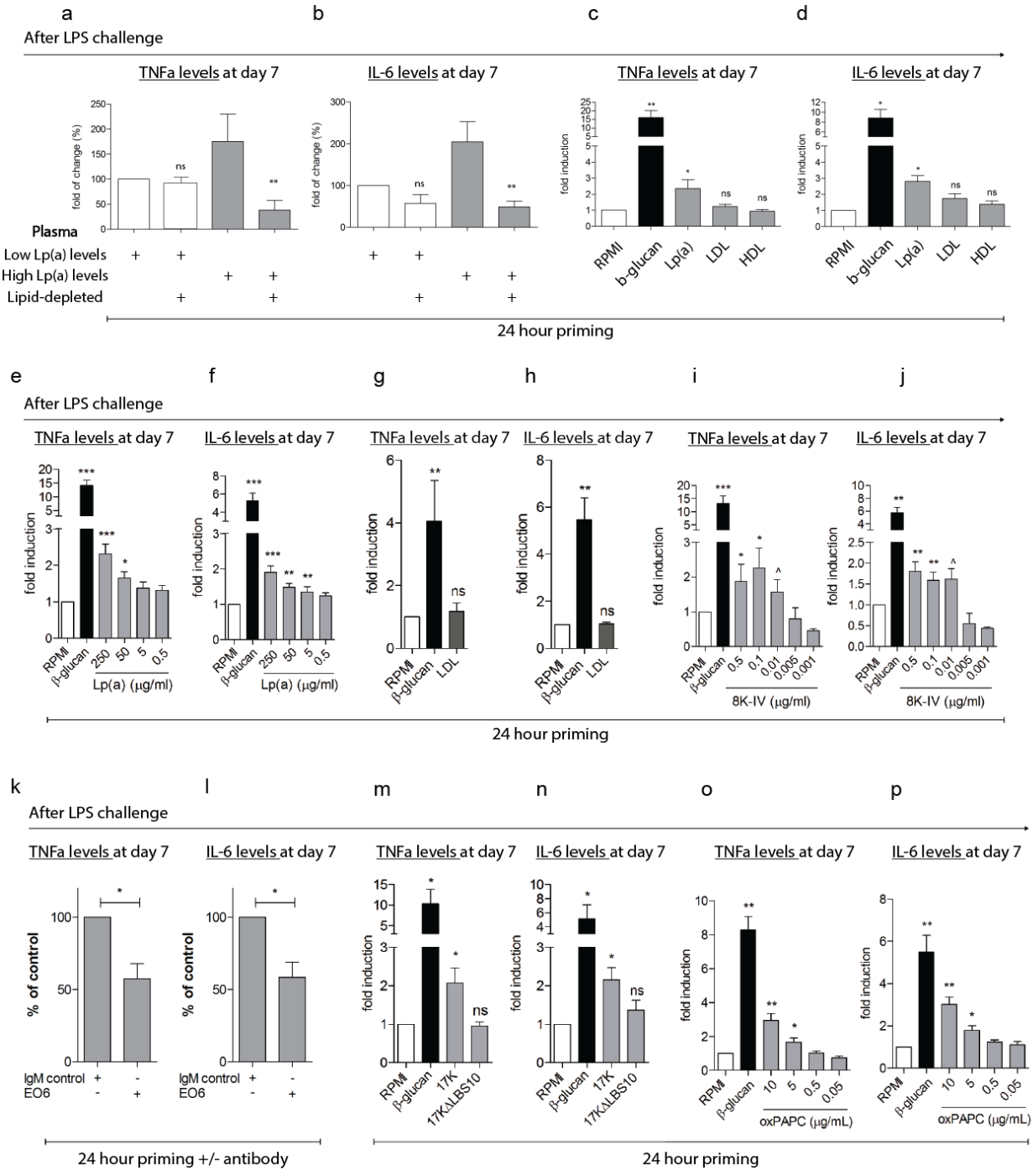

(**A,B**) priming healthy monocytes with plasma with high Lp(a) (grey bars) for 24h resulted in an increased production of TNFα and IL-6 upon re-stimulation with LPS (10 ng/mL) on day 6, compared with plasma of normal Lp(a) (white bars). In addition, after lipid-depletion this effect

was profoundly reduced (n=3), (**C,D**) priming of healthy monocytes with β-glucan (5 μg/mL, positive control, black bar) or Lp(a) (grey bar, 250 μg/mL) for 24h, induced an increased production of TNFα and IL-6 upon re-stimulation with LPS (10 ng/mL) on day 6, compared with priming with RPMI (negative control, white bar), LDL (grey bar, 10 μg/mL) or HDL (grey bar, 10 μg/mL) (n=6), (**E,F**) in addition we show a dose-dependent increased production of TNFα and IL-6 after LP(a) priming, upon re-stimulation with LPS (10 ng/mL) on day 6, compared with priming with RPMI (negative control, white bar) (n=6), (**G,H**) priming with LDL (10 μg/mL, grey bar) did not increase cytokine production after LPS (10 ng/mL) (n=6), (**I,J**) priming of healthy monocytes with β-glucan (5 μg/mL, positive control, black bar) or the r-apo(a) construct, 8K-IV, (grey bars) increased TNFα and IL-6 production after LPS (10 ng/mL) (n=6), compared to RPMI (negative control, white bar), (**K,L**) pre-treatment with the E06 antibody (1 nM) against OxPL inhibited the priming effects of 8K-IV (0.1 μg/mL, grey bars), whereas IgM (1 nM) did not (n=6), (**M,N**) β-glucan (5 μg/mL, positive control, black bar) and the r-apo(a) construct 17K priming (0.1 μg/mL grey bar) increased cytokine production upon LPS (10 ng/mL), whereas 17KΔLBS lacking OxPL (0.1 μg/mL, grey bar) did not (n=6), (**O,P**) priming with β-glucan (5 μg/mL, positive control, black bar) and oxPAPC (grey bars) increased the monocyte response upon LPS (10 ng/mL) compared to RPMI (negative control, white bar) (n=6). ^=*p<0.06, *=p<0.05, **=p<0.01, ***=p<0.001*

Video Files

Movie S1. Migration of monocytes of subjects with elevated Lp(a) and normal Lp(a)

Freshly isolated monocytes of subjects with elevated Lp(a) have increased monocyte motility compared to monocytes of subjects with normal Lp(a) when plated on a fibronectin matrix, whereas isolated monocytes of subjects with normal Lp(a) display less monocyte motility.

References applied to supplementary

1. Folch J, Lees M, Sloane Stanley G. A simple method for the isolation and purification of total lipides from animal tissues. *The Journal of biological chemistry*. 1957;226:497-509

2. White CW, Hasanally D, Mundt P, Li Y, Xiang B, Klein J, Muller A, Ambrose E, Ravandi A, Arora RC, Lee TW, Hryshko LV, Large S, Tian G, Freed DH. A whole blood-based perfusate provides superior preservation of myocardial function during ex vivo heart perfusion. *The Journal of heart and lung transplantation : the official publication of the International Society for Heart Transplantation*. 2015;34:113-121

3. Gruber F, Bicker W, Oskolkova O, Tschachler E, Bochkov V. A simplified procedure for semi-targeted lipidomic analysis of oxidized phosphatidylcholines induced by uva irradiation. *Journal of lipid research*. 2012;53:1232-1242

4. Vo MN, Brilakis ES, Kass M, Ravandi A. Physiologic significance of coronary collaterals in chronic total occlusions. *Canadian journal of physiology and pharmacology*. 2015;93:867-71.

5. Zeglinski M, Premecz S, Lerner J, Wtorek P, Dasilva M, Hasanally D, Chaudhary R, Sharma A, Thliveris J, Ravandi A, Singal PK, Jassal DS. Congenital absence of nitric oxide synthase 3 potentiates cardiac dysfunction and reduces survival in doxorubicin- and trastuzumab-mediated cardiomyopathy. *The Canadian journal of cardiology*. 2014;30:359-367

6. Hasanally D, Chan D, Chaudhary R, Margulets V, Premecz S, Kirshenbaum LA, Jassal DS, Ravandi A. Novel bioactive oxidized phospholipids are produced in myocardium during ischemia reperfusion and act as mediators of cell death within cardiac myocytes. *European Heart Journal*. 2014;35:306-306

7. Ravandi A, Leibundgut G, Hung MY, Patel M, Hutchins PM, Murphy RC, Prasad A, Mahmud E, Miller YI, Dennis EA, Witztum JL, Tsimikas S. Release and capture of bioactive

oxidized phospholipids and oxidized cholesteryl esters during percutaneous coronary and peripheral arterial interventions in humans. *Journal of the American College of Cardiology*. 2014;63:1961-1971

8. Bordun KA, Premecz S, daSilva M, Mandal S, Goyal V, Glavinovic T, Cheung M, Cheung D, White CW, Chaudhary R, Freed DH, Villarraga HR, Herrmann J, Kohli M, Ravandi A, Thliveris J, Pitz M, Singal PK, Mulvagh S, Jassal DS. The utility of cardiac biomarkers and echocardiography for the early detection of bevacizumab- and sunitinib-mediated cardiotoxicity. *American journal of physiology. Heart and circulatory physiology*. 2015;309:H692-701

9. Yamaguchi T, Devassy JG, Gabbs M, Ravandi A, Nagao S, Aukema HM. Dietary flax oil rich in alpha-linolenic acid reduces renal disease and oxylipin abnormalities, including formation of docosahexaenoic acid derived oxylipins in the cd1-pcy/pcy mouse model of nephronophthisis. *Prostaglandins, leukotrienes, and essential fatty acids*. 2015;94:83-89